Organo-Aluminum and Zinc Acetamidinates:

Preparation, Coordination Ability and ROP Processes of

Cyclic Esters

Andrés Garcés,[†] Luis F. Sánchez-Barba,*,[†] Juan Fernández-Baeza,[‡] Antonio Otero,*,[‡] Israel Fernández,[§] Agustín Lara-Sánchez,[‡] and Ana M. Rodríguez[‡]

[†]Departamento de Biología y Geología, Física y Química Inorgánica, Universidad Rey Juan Carlos, Móstoles-28933-Madrid, Spain.

[‡]Universidad de Castilla-La Mancha, Departamento de Química Inorgánica, Orgánica y Bioquímica-Centro de Innovación en Química Avanzada (ORFEO-CINQA), Campus Universitario, 13071-Ciudad Real, Spain.

[§]Departamento de Química Orgánica I-Centro de Innovación en Química Avanzada (ORFEO-CINQA), Facultad de Ciencias Químicas, Universidad Complutense de Madrid, 28040, Madrid, Spain.

E-mail: luisfernando.sanchezbarba@urjc.es, antonio.otero@uclm.es;

RECEIVED DATE (to be automatically inserted after your manuscript is accepted if required according to the journal that you are submitting your paper to)

ABSTRACT

The reaction of the highly sterically demanding NNN'-heteroscorpionate protioligands pbp^{t}amd-H, tbp^{t}amd-H and phbp^{t}amd-H (**a**) and the low sterically hindered analogs pbpamd-H, tbpamd-H and phbpamd-H (**b**), with 1 equiv of AlR$_3$ (R = Me, Et) proceed in high yields to give two families of complexes; the mononuclear dialkyl aluminum bidentate-acetamidinates [AlR$_2$(κ^2-N'N')] (κ^2-N'N' = pbp^{t}amd, R = Me **1**, Et **2**; tbp^{t}amd, R = Me **3**, Et **4**; phbp^{t}amd, R = Me **5**, Et **6**) and the monodentate-acetamidinates [AlR$_2$(κ^2-NN')] (κ^2-NN' = tbpamd, R = Me **7**; phbpamd, R = Me **8**, Et **9**). In complexes **7**–**9** the presence of two possible CH–NH tautomers as low extended π-N−C−N'(sp^2)−Al and large extended π-HN−C$_2$−N'(sp^2)−Al complexes, respectively, could be identified. Moreover, the reaction of the aluminum dimethyls **7** and **8** with ZnMe$_2$ afforded the isolation of the more stable scorpionate zinc monoalkyls [Zn(Me)(κ^3-NNN')] (NNN' = tbpamd **10** and phbpamd **11**), through a very unusual ligand exchange process, involving a zinc-to-aluminum transmetalation of an alkyl group. The X-ray crystal structures of **1**, **3**, **7** and **8**, as well as **11** confirmed unambiguously the different κ^2-arrangements proposed for the acetamidinate bi- or monodentate dialkyls **1**–**6** and **7**–**9**, respectively, the presence of the NH tautomer in **7** and **8**, and a κ^3-NNN' coordination in the monoalkyl **11**. DFT calculations were used to explore the three different favored κ^2-arrangements found in the acetamidinate aluminum dialkyls **1**–**9**, the relative stability of both CH–NH tautomers, and the ligand transfer reaction leading to the formation of the κ^3-NNN' zinc monoalkyls **10** and **11**.

Interestingly, the dialkyls **1**, **5**, **7** and **8** can act as highly efficient single-component living initiators for the ROP of ε-caprolactone and *rac*-lactide in mild conditions after hours. These initiators efficiently mediated the immortal polymerization in the presence of excess of benzyl alcohol (up to 20 equiv), as evidenced by the narrow dispersity values and the good agreement between the experimental M_n values and monomer/benzyl alcohol ratios. In addition, the most sterically hindered initiator **5** exhibits enhanced levels of heteroselectivity on the produced PLAs, reaching P_s values up to 0.70.

Introduction

Over the last decade, the Ring-Opening Polymerization (ROP) of bio-renewable cyclic esters has attracted great attention[1,2] as a result of the important concerns about the environmental problems and the depletion of fossil fuel feedstocks. In this regard, the polylactide (PLA)[3] is a top commercial biosourced material, which is annually increasing its production, being estimated the 7% of the total bioplastics worldwide production in 2021.[4] PLAs can be in fact prepared by using non-hazardous well-defined metallic initiators through a coordination–insertion mechanism, with good control of molecular weight, molecular weight distribution and stereoselectivity. This procedure constitutes a much greener alternative to the toxic industrially employed tin(II) 2-ethylhexanoate, which, additionally, poorly controls the above-mentioned parameters in the resulting materials.

In this context, its biodegradability and biocompatibility make PLA an attractive material not only for biomedical and pharmaceutical applications such as regenerative medicine,[5] controlled release of drugs[6] and wound healing,[7a] but also for its broad use in packaging and agriculture as ideal alternatives to conventional commodity thermoplastics.[7b] For this reason, biologically benign metal-based catalysts are of great interest for the production of this bioassimilable material, with zinc,[8] magnesium[9] and calcium[10] as leading metals, in addition to the important participation of aluminum,[11] and group 4[12] and 13[13] metals, as well as rare earth[14] metals, which have incorporated a rich variety of ligands.

In this sense, our research group has been investigating in the recent years the employment of well-defined multinuclear organo-zinc,[15] -magnesium[16] and -aluminum[17] complexes supported by scorpionate ancillary ligands $[M(R)(\kappa^n\text{-NNX})]$ (M = Mg, Zn, n = 3, X = N, O; M = Al, n = 2, X = O, S; R = alkyl, alkoxide, amide) as efficient single-component living initiators for the ROP of cyclic esters.[18] Thus, from moderate to significant levels of heterotacticity ($P_s = 0.78-0.85$)[16] and isotacticity ($P_i = 0.77$)[15] have been reached using magnesium- and zinc-based initiators, whereas in the case of aluminum, the successful production of linear and cyclic poly(ε-caprolactone)s (PCLs), copolymers of CL and L-LA, as well as poly(L-/*rac*-lactide)s were reached.[17] However, after employing energic conditions, no significant levels of stereoselectivity in the *rac*-PLAs produced were achieved.

In contrast, very effective aluminum-based systems have been reported in the literature for the ROP of *rac*-LA. For instance, Chakraborty[19a] and Du[19b] *et al*. have recently described efficient aluminum catalysts bearing *N,O*-aminophenol or anilido-oxazolinate ligands, and Kol[20] *et al*. have recently communicated aluminum systems supported by salan ligands, which provided heterotactic control in the polymerization process, reaching P_s values up to 0.74 (100 ºC, 18 h)[19] and 0.98 (50 ºC, 12 h),[20] respectively.

Alternatively, Lin *et al*.[21] employed aluminum alkoxides coordinated on salen-type ancillary ligands for the successful production of isotactic highly enriched PLAs, (P_i = 0.94-0.97, 12-55 h, 70ºC), simultaneously to Williams *et al*.[22] who reported bis(8-quinolinolato)aluminum ethyl complexes as iso-selective initiators (P_i = 0.76, 36 h, 70ºC). Very recently, Hormnirun *et al*. also reported aluminum alkyls supported by salicylbenzoxazole[23a] and salicylbenzothiazole[23b] ligands for the production of isotactic enriched poly(*rac*-lactide)s (P_i ≈ 0.75, 36 h, 70ºC; P_i ≈ 0.66, 96 h, 70ºC, respectively), and bis(pyrrolidene) schiff base aluminum complexes[23c] for the production of isotactic stereoblocks (P_i = 0.80, 1h, 70ºC). In addition, Jones *et al*.[23d] have communicated salan aluminum initiators based on the 2-aminopiperidine ligand (P_i = 0.83, 120 h, 80ºC). However, in all cases high temperatures were necessary to reach almost complete conversions in combination with long periods of time in many cases.

In addition to this, the low toxicity of aluminum[24] in conjunction with its low-cost, high Lewis acidity and redox-inactivity, make this metal of particular interest for this polymerization purpose, and therefore, we take now the challenge to design more active and stereoselective organoaluminum initiators, alternatives to these of Zn,[15] Mg[16] and Al[17] described in our group, and those reported in the literature.[19-23]

We report hereby the preparation of new mononuclear aluminum dialkyls supported by low and high sterically hindered acetamidinate-based scorpionates. The different κ^2-arrangements observed, the two CH–NH tautomers formed in conjunction with the very unusual ligand exchange processes *versus* ZnMe₂, have been also corroborated by DFT calculations. In addition, their performance in the ROP of ε-CL and *rac*-LA as efficient single-component living and immortal initiators to produce heteroenriched PLAs was also investigated in detail.
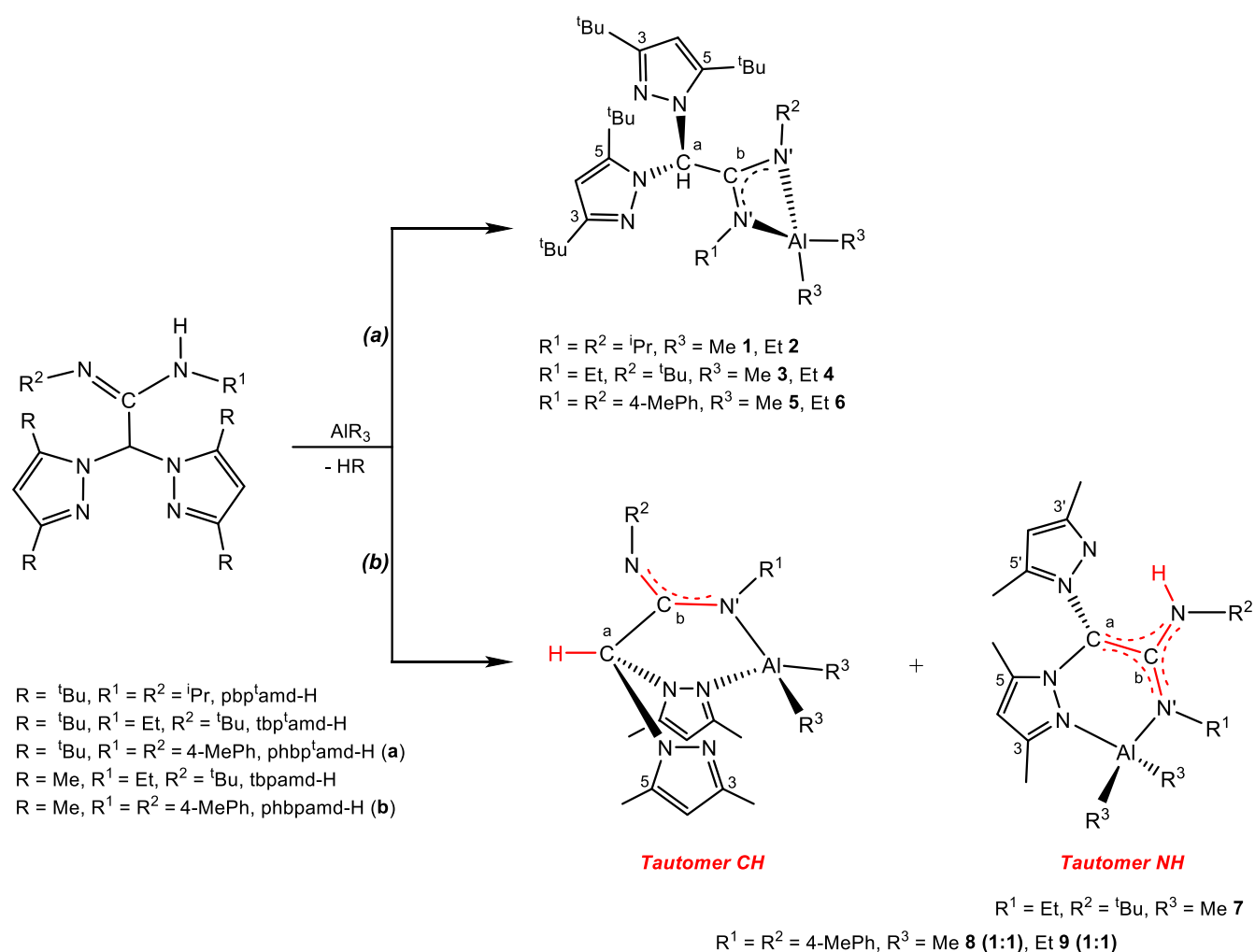
Results and Discussion

Synthesis and Characterization of Dialkyl Aluminum Complexes (1–9).

In a similar manner as previously described,[25] the hydrolysis of the high and low sterically congested scorpionate lithium salts [Li(phbp^{t}amd)(THF)] [phbp^{t}amd = *N,N'*-di-*p*-tolylbis(3,5-di-*tert*-butylpyrazole-1-yl)acetamidinate] and [Li(phbpamd)(THF)] [phbpamd = *N,N'*-di-*p*-tolylbis(3,5-dimethylpyrazole-1-yl)acetamidinate], respectively, with NH$_4$Cl/H$_2$O in diethyl ether cleanly affords the corresponding new acetamidine scorpionate protioligands Hphbp^{t}amd (**a**) [Hphbp^{t}amd = *N,N'*-di-*p*-tolylbis(3,5-di-*tert*-butylpyrazole-1-yl)acetamidine] and Hphbpamd (**b**) [Hphbpamd = *N,N'*-di-*p*-tolylbis(3,5-dimethylpyrazole-1-yl)acetamidine] (see Scheme 1). The ^{1}H and ^{13}C{^{1}H} NMR spectra of the acetamidine-scorpionates **a** and **b** presented a similar pattern to the previously reported analogs.[25] The X-ray molecular structure of **b** was determined and is showed in the Supporting Information (SI) in the X-ray diffraction studies section.

Subsequent protonolysis reaction of the high sterically demanded acetamidinate-based scorpionate protioligands[25] Hpbp^{t}amd (Hpbp^{t}amd = *N,N'*-diisopropylbis(3,5-di-*tert*-butylpyrazole-1-yl)acetamidine), Htbp^{t}amd (Htbp^{t}amd = *N*-ethyl-*N'*-*tert*-butylbis(3,5-di-*tert*-butylpyrazole-1-yl)acetamidine), and Hphbp^{t}amd (**a**), and their low sterically hindered analogues[25] Htbpamd (Htbpamd = *N*-ethyl-*N'*-*tert*-butylbis(3,5-dimethylpyrazole-1-yl)acetamidine), and Hphbpamd (**b**) with AlR$_3$ (R = Me, Et) in toluene at room temperature afforded the corresponding aluminum acetamidinate bidentate dialkyls [AlR$_2$(κ^2-N'N')] (**1–6**) (κ^2-N'N' = pbp^{t}amd, R = Me **1**, Et **2**; tbp^{t}amd, R = Me **3**, Et **4**; phbp^{t}amd, R = Me **5**, Et **6**) (see Scheme 1a), and the aluminum acetamidinate monodentate dialkyls [AlR$_2$(κ^2-NN')] (**7–9**) (κ^2-NN' = tbpamd, R = Me **7**; phbpamd, R = Me **8**, Et **9**) (see Scheme 1b), as white solids in very high yields (~85%) after the appropriate workup. The dialkyl **7** was obtained as a single N–H tautomeric form, while **8** and **9** presented an equimolecular mixture of the N–H and C–H tautomers (see Scheme 1b). The

preparation of the N–H tautomer is rather surprising since their formation implies an apical C−H methine activation on the scorpionate ligand in such a way that the hydrogen atom initially attached to the bridging C^a of the C–H tautomeric form has clearly migrated to the nitrogen atom of the imine center. To best of our knowledge, this outcome has never been observed before in the chemistry of scorpionate complexes. All compounds **1–9** resulted highly air- and moisture-sensitive, and readily decomposed when dissolved in dichloromethane.

Scheme 1. Preparation of the acetamidinate aluminum dialkyls (1–9)

$R^1 = R^2 = {}^iPr, R^3 = Me$ **1**, Et **2**
$R^1 = Et, R^2 = {}^tBu, R^3 = Me$ **3**, Et **4**
$R^1 = R^2 = 4\text{-MePh}, R^3 = Me$ **5**, Et **6**

(a)

(b)

$R = {}^tBu, R^1 = R^2 = {}^iPr,$ pbp^{t}amd-H
$R = {}^tBu, R^1 = Et, R^2 = {}^tBu,$ tbp^{t}amd-H
$R = {}^tBu, R^1 = R^2 = 4\text{-MePh},$ phbp^{t}amd-H (**a**)
$R = Me, R^1 = Et, R^2 = {}^tBu,$ tbpamd-H
$R = Me, R^1 = R^2 = 4\text{-MePh},$ phbpamd-H (**b**)

Tautomer CH   *Tautomer NH*

$R^1 = Et, R^2 = {}^tBu, R^3 = Me$ **7**
$R^1 = R^2 = 4\text{-MePh}, R^3 = Me$ **8** (1:1), Et **9** (1:1)

The ^{1}H and ^{13}C {^{1}H} NMR spectra of **1−9** in benzene-d_6 at room temperature show different patterns. The spectra of the complexes **1−6** show two sets of resonances for the sterically hindered pyrazole rings at similar fields to the corresponding ligands, suggesting both magnetic inequivalence and uncoordination

in the pyrazole rings, and two close signals for the acetamidinate fragments in **1−2** and **5−6**, which are in agreement with a bidentate binding for the acetamidinate moiety, on the basis of the rotation restrictions in the pyrazole rings due to their sterically hindered environment (see Scheme 1a). Two signals at negative chemical shift appear for both alkyl groups (see Figure S1 in the SI).

The N–H tautomer in the complexes **7−9** present two sets of resonances for the inequivalent pyrazole rings, but in this case, the shifting of the $Me^{3,5}$ signals from one pyrazole ring to lower fields evidences coordination to the metal. Moreover, two separated sets of resonances were found for the acetamidinate fragment in **8** and **9**, suggesting a monodentate binding mode (see Scheme 1b). In addition, one and two signals are observed for both the N−H proton and both alkyl groups, respectively (see Figure S2 in the SI).

Nonetheless, the C–H tautomer in the complexes **8** and **9** shows in their spectra one signal for the CH group, as well as a single set of resonances for the pyrazole rings, probably due to that an exchange process between one coordinated and one uncoordinated pyrazole rings occurs at room temperature, being too fast to be detected on the NMR time scale. This finding suggests that interconversion from one proposed stereoisomer to the other takes place (see Figure S3 in the SI), and as a consequence, both proposed stereoisomers appear equivalent. VT NMR analysis in toluene-d_8 of complex **9** confirmed the proposed exchange process in such a way that the coalescence temperature for the interconversion between both stereoisomers is −40ºC, much higher than that found in analogs scorpionate aluminum dialkyls (−90ºC),[17] very likely due to the high steric restrictions produced by the acetamidinate phenyl substituents in **9** (see Figure S4 in the SI). In addition, the presence of two separated sets of resonances for the acetamidinate fragment in both complexes (see Figure S5 in the SI) supports the proposed structural disposition with a monodentate coordination mode of the acetamidinate (see Scheme 1b), and accordingly, the acetamidinate bidentate coordination mode, as observed in complexes **1−6**, can be discarded. This type of scorpionate coordination mode has commonly been observed in our group previously.[17] Additionally, for these CH tautomers only one signal at negative chemical shift appears for both alkyl groups (see Figure S5 in the SI).

Interestingly, the C^a and C^b shifts in the ^{13}C {^1H} NMR spectra for the N−H tautomer *versus* the corresponding ones in the C−H tautomer for complexes **8** and **9** are notably modified. Thus, while the C^a is shifted to lower fields (from ~70 ppm to ~105 ppm), C^b appears at higher fields (from ~160 ppm to ~150 ppm). These results are due to the change of hybridization at the C^a atom from formally sp^3 to sp^2 in conjunction with the electron rearrangement present over the whole π-HN−C_2−N'(sp^2) fragment of the N−H tautomers (see Scheme 1b).

In addition, we found interesting to study the possibility of dependence in the proportion of the tautomers with time and/or temperature. Thus, we observe in the case of **7** that after only 1 hour of reaction in hexane, the initial CH−NH tautomer mixture presents a 60:40 proportion (see Figure S6a in the SI), and after 10 additional hours, the ratio progresses with enrichment on the N−H tautomer up to 40:60 (see Figure S6b in the SI), leading to a complete conversion process after 24 hours (see Figure S6c in the SI). Alternatively, the N−H tautomer can be directly obtained by simply heating the initial solution up to 80 ºC for 1 hour, as described in the Experimental Section, showing the additional temperature dependence of this process. Moreover, no modification on the 50:50 proportion of CH−NH tautomers in the cases of **8** and **9** could be observed with either time or temperature.

To confirm the arrangements proposed for the dialkyl complexes **1−9**, ^1H NOESY-1D experiments were performed, which also allowed us to unambiguously assign each signal in all complexes. In addition, the signals for C^4, $Me^{3,5}$ and $^tBu^{3,5}$ in the pyrazole rings, as well as R, R^1, R^2 and R^3 in all compounds were assigned by ^1H−^{13}C heteronuclear correlations (g-HSQC). The proposed structures for the acetamidinate bidentate dialkyls (**1−6**), and the N−H tautomer of the acetamidinate monodentate dialkyls (**7−9**) were further confirmed by the X-ray molecular analysis (see below Figures 1 and 2) and agreed by DFT calculations.

Single crystals of the protioligand phbpamd-H (**b**), the complexes **1**, **3**, and the N–H tautomers of **7** and **8** suitable for X-ray diffraction were easily grown from toluene or hexane solutions at –26 ºC. In the case of **8**, the ^1H NMR of the mother liquor in the crystals sample showed the remaining CH tautomer as the main species. The molecular structures of **1** and **7** are depicted in Figures 1 and 2, respectively, and the

structures of **b**, **3** and **8** are shown in Figures S7–S9 in the Supporting Information (SI), respectively. Selected bond lengths and angles are collected in Table 1 for **1** and **7**, and in Table S1 in the SI for **b**, **3** and **8**. Crystallographic details for all crystal structures are reported in Table S3 in the SI.

The dialkyl complexes **1**, **3**, **7** and **8** exhibit a monomeric mononuclear unit in the solid state and contain a distorted tetrahedral aluminum center. Interestingly, in complexes **1** and **3** the acetamidinate ligands are in a κ^2-N',N' acetamidinate bidentate coordination mode and occupy two positions around the metal. The N(5)–Al(1) and N(6)–Al(1) bond lengths [*i. e.*: 1.9439(19) Å and 1.945(2) Å for **1**] are well-balanced and compare well between them. In addition, complexes **1** and **3** show in the N(5)–C(12)–N(6) fragment nearly identical delocalization, with bond distances of N(5)–C(24) = 1.3265(19)–1.337(3) Å and N(6)–C(24) = 1.330(3)–1.3373(19) Å. It is worth noting the bond distances Al(1)–C(24) for the two complexes of 2.354(2)–2.357(3) Å, in which an additional bond interaction cannot be ruled out.[26] The two additional positions around the aluminum atom are occupied in both complexes by an alkyl group, with almost identical Al–C bond distances [Al(1)–C(31 or 32) = 1.9616(18)–1.972(3) Å]. Both complexes present a C(23)–C(24) bond distance of 1.542(19)–1.544(3) Å, which clearly corresponds to a C–C simple bond (~1.54 Å). These bond lengths are consistent with those previously observed in analogs scorpionate aluminum alkyls.[17a]

Furthermore, the N–H tautomeric forms for complexes **7** and **8** also present the ligands coordinated in a κ^2-N,N' fashion, but in this case, through one nitrogen from the acetamidinate fragment, and only one pyrazole ring, N(1) and N(5), respectively, with Al(1)–N(5) bond distances shorter [1.862(2) Å **7**; 1.899(2) Å **8**] than the Al(1)–N(1) distances [1.963(2) Å **7**; 1.966(2) Å **8**]. This κ^2-N,N' acetamidinate monodentate coordination mode offers a wider angle between the aluminum and the nitrogen atoms than that for the κ^2-N',N', in an acetamidinate bidentate fashion [N(5)−Al(1)−N(6) = 68.75(8)°–68.91(5)° for **1** and **3**, respectively, *versus* N(5)−Al(1)−N(1) = 94.23(8)°–95.57(8)° for **7** and **8**, respectively].

More interestingly, the planar geometry of both C(11) and C(12), with angles around the central C(11) [*i. e.*: N(2)−C(11)−N(4) = 113.51(16)°, N(2)−C(11)−C(12) = 123.1(2)° and N(4)−C(11)−C(12) =

123.34(19)º for **7**], and around the central C(12) [*i. e.*: N(5)−C(12)−N(6) = 120.77(18)º, N(5)−C(12)−C(11) = 121.21(19)º and N(6)−C(12)−C(11) = 117.98(19)º for **7**], close to 120º, is consistent with a sp^2 hybridization for both carbon atoms C(11) and C(12), and in conjunction with the C(11)–C(12) bond distances of 1.361(3) Å and 1.359(3) Å for **7** and **8**, respectively, evidence the almost pure double character of this C–C bond (~1.34 Å), as a result of the N–H tautomer formation.

In addition, the N(5)–C(12)–N(6) moiety presents nearly equal bond distances [N(5)–C(12) = 1.357(3) Å and 1.380(3) Å, and N(6)–C(12) = 1.398(3) Å and 1.382(3) Å, for **7** and **8**, respectively], shorter than that for a simple C–N bond [1.46–1.48 Å], indicating almost symmetrical delocalization of the additional electron density throughout the acetamidinate fragment, which forces nitrogen atoms N(5) and N(6) to adopt sp^2–hybridization, as evidenced by both the angles around the central N(5) and N(6) [*i. e.*: C(12)−N(5)−C(13) = 118.0(2)º, C(13)−N(5)−Al(1) = 123.61(15)º, C(12)−N(5)−Al(1) = 118.19(14)º and C(12)−N(6)−C(15) = 121.09(16)º for **7**] close to 120º, and the coplanarity of the substituents on each amidine nitrogen in both complexes. As a result of this electron density distribution, a large extended π-HN(6)−C$_2$(11,12)−N(5)(sp^2) fragment is stablished in the N–H tautomeric forms (see Scheme 1).

As far as we know, only one example of this class of this large extended π-HN−C$_2$−N'(sp^2) has been described by Schulz *et al.*[27] Two additional methyl groups occupy the final positions around the aluminum atom, with almost equivalent Al–C bond distances [Al(1)–C(19,20,27,28) = 1.958(3)–1.959(3) Å]. These N–H tautomer crystal structures are further stabilized by two additional NH···CH-π intermolecular contacts for **7**, and one N–H···N intramolecular hydrogen bond of 2.28(2) Å for **8**.
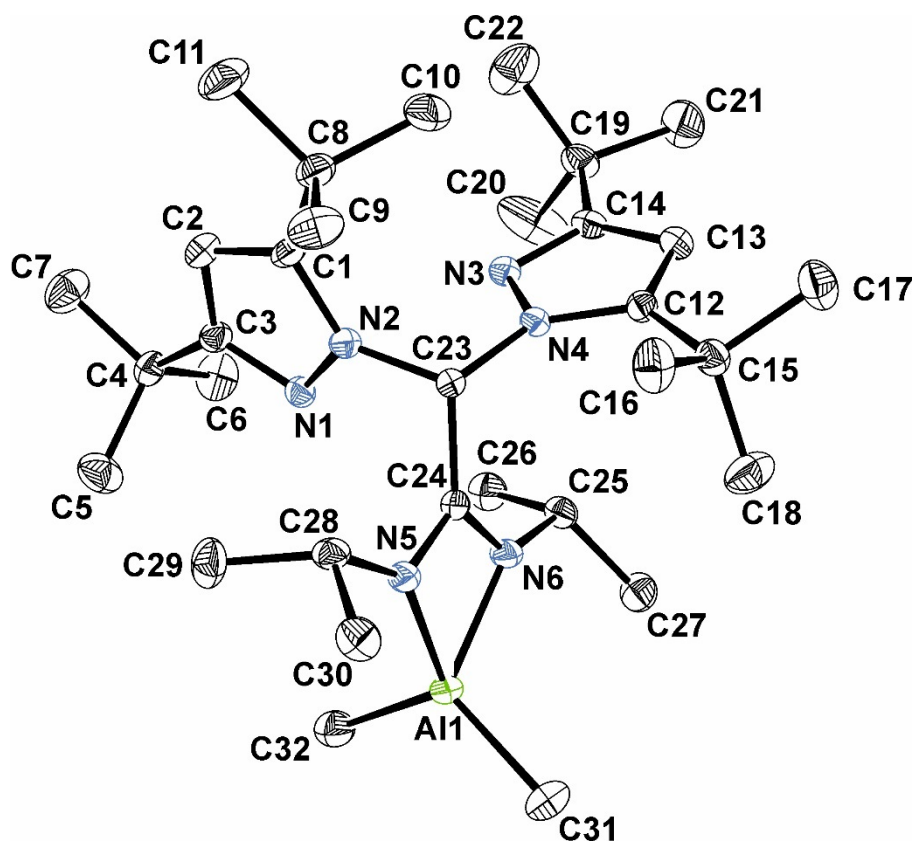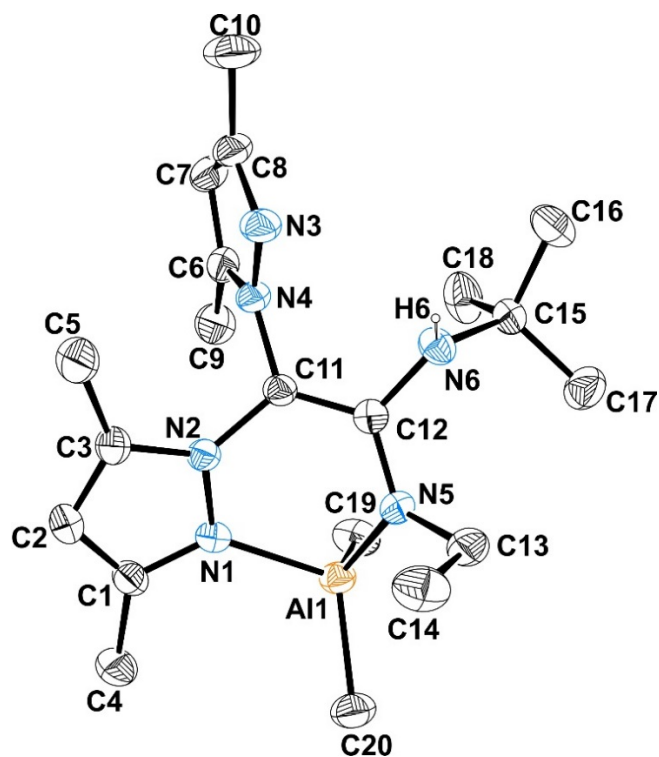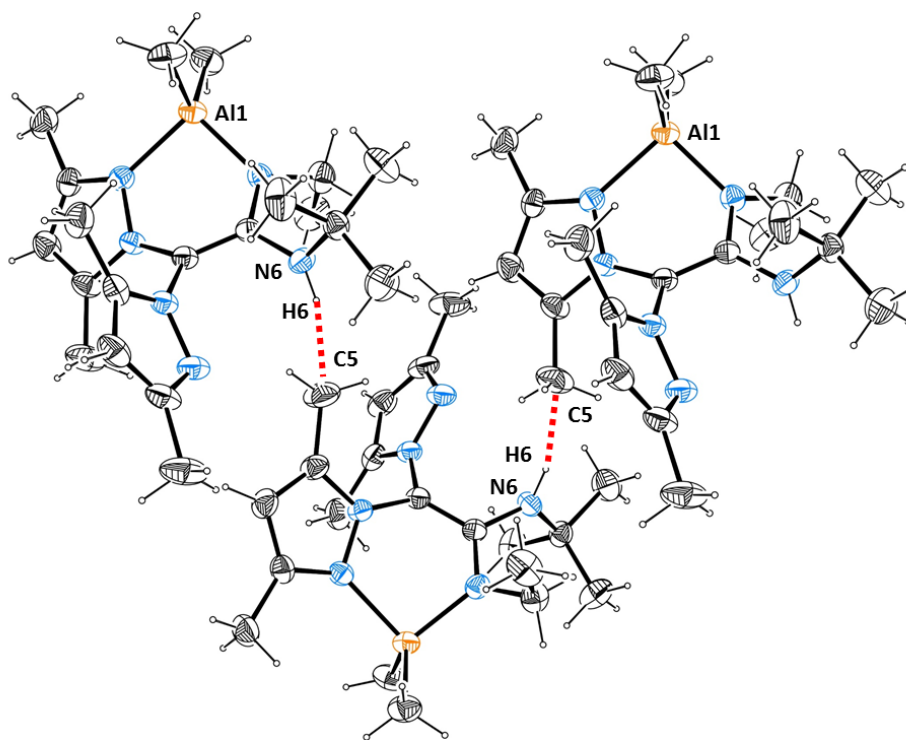
Figure 1. ORTEP view of [Al(Me)$_2$(κ^2-pbp^{t}amd)] (**1**). Hydrogen atoms have been omitted for clarity. Thermal ellipsoids are drawn at the 30% probability level.

(a)

(b)

Figure 2. (a) ORTEP view of [Al(Me)$_2$(κ^2-tbpamd)] (**7**). Hydrogen atoms have been omitted for clarity.

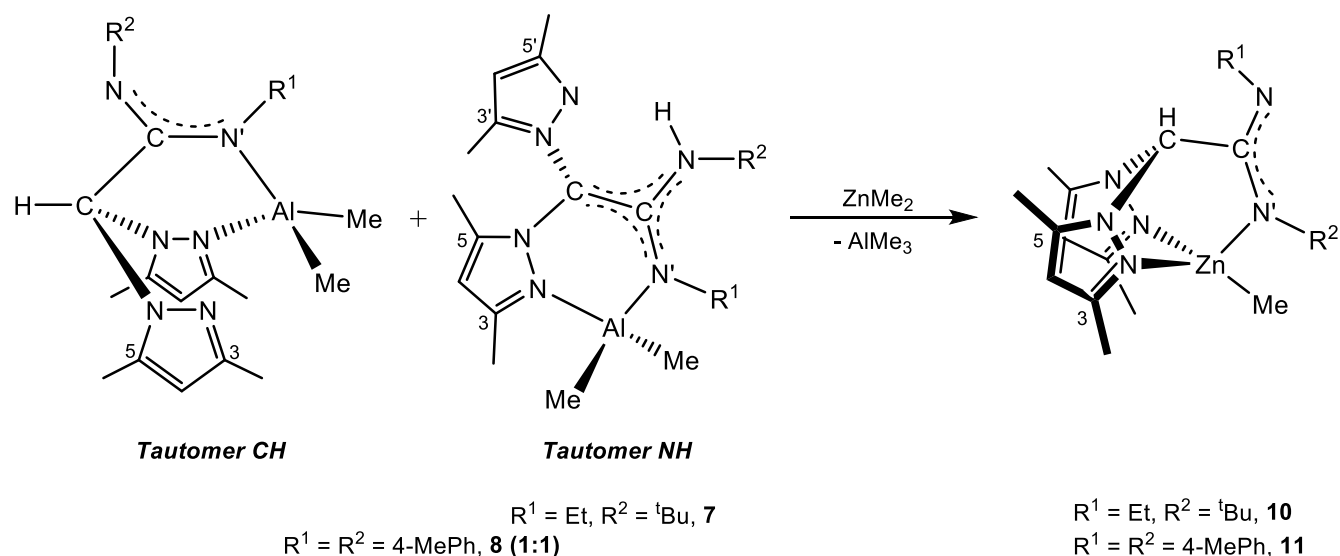Thermal ellipsoids are drawn at the 30% probability level. (b) NH···CH-π intermolecular contacts.

Considering the structural arrangements found in the aluminum dialkyls $[AlR_2(\kappa^2\text{-N'N'})]$ (**1**–**6**) and $[AlR_2(\kappa^2\text{-NN'})]$ (**7**–**9**) described above, where two (**1**–**6**) or one (**7**–**9**) pyrazole rings remain uncoordinated, we focused this time on the possibility to generate heterobimetallic species by simple addition of $ZnMe_2$ to these aluminum species and subsequent coordination to the pyrazole rings through the pyridinic nitrogen atoms. With this purpose, several really interesting works have very recently appeared[28] describing the cooperative effect of two remote metal atoms, including aluminum,[28a] zinc[28b,c] or titanium,[28d] in homo-binuclear species for the ROP of cyclic esters such as ε-caprolactone and lactides. In this case, we alternatively planned to study the effect of two different remote metal centers on the ROP of *rac*-LA.

Thus, we proved the test reaction of the dimethyls $[Al(Me)_2(\kappa^2\text{-tbpamd})]$ (**7**) and $[Al(Me)_2(\kappa^2\text{-phbpamd})]$ (**8**) with $ZnMe_2$ (since this zinc reagent is the easiest one to be followed by ^{1}H-NMR) during 18 h in toluene at 20ºC. Unfortunately, we did not reach our original propose, but quite surprisingly, we obtained the corresponding monoalkyl zinc scorpionate complexes $[Zn(Me)(\kappa^3\text{-NNN'})]$ (**10**–**11**) (κ^3-NNN' = tbpamd **10** and phbpamd **11**), through a very unusual exchange reaction of the ancillary scorpionate ligand, including a zinc-to-aluminum transmetalation alkyl group (see Scheme 2).

We have previously observed a similar ligand exchange reaction between the hybrid scorpionate/cyclopentadienyl magnesium alkyls $[Mg(R)(\kappa^2\text{-}\eta^5\text{-bpzcp})]$ with $ZnCl_2$ to yield the corresponding zinc alkyl analogs of the type $[Zn(R)\{\kappa^2\text{-}\eta^1(\pi)\text{-bpzcp}\}]$;[29] however, as far as we are conscious, this type of ligand transfer reaction between aluminum and zinc alkyls are very unusual, and only one example of this aluminium-to-zinc transmetalation have been previously reported.[30] We hypothesize that the driving force for this unexpected transfer reaction is the formation of more stable κ^3-NNN' tridentate zinc methyl complexes $[Zn(Me)(\kappa^3\text{-NNN'})]$ (**10**–**11**) *versus* the starting κ^2-NN' acetamidinate mono- and κ^2-N'N' bidentate aluminum dimethyl species **7** and **8**.

Scheme 2. Preparation of the acetamidinate-based scorpionate monoalkyl zinc complexes 10 and 11 by a ligand exchange process.

Tautomer CH   Tautomer NH

R^1 = Et, R^2 = ^{t}Bu, **7**
R^1 = R^2 = 4-MePh, **8 (1:1)**

R^1 = Et, R^2 = ^{t}Bu, **10**
R^1 = R^2 = 4-MePh, **11**

The ^{1}H and ^{13}C {^{1}H} NMR spectra of **10** and **11** in benzene-d_6 at room temperature show a single set of resonances for the pyrazole rings. The acetamidinate moiety, with R$_1$ = Et and R$_2$ = ^{t}Bu (**10**), as well as R$_1$ = R$_2$ = Ph (**11**) gives rise two sets of resonances for these two substituents, indicating a monodentate binding coordination of this fragment to the zinc center (see Scheme 2). One signal at negative chemical shift is also observed corresponding to the methyl group in all cases. ^{1}H NOESY-1D experiments confirm the arrangement proposed for this family of zinc alkyls, and the signals for C^4 and Me^{3,5} in the pyrazole rings, as well as R^1, R^2 and the methyl groups in all compounds were assigned by ^{1}H–^{13}C heteronuclear correlations (g-HSQC). The structures proposed were further confirmed by the X-ray studies below (see below Figure 3) and corroborated by DFT calculations.

Single crystals X-ray diffraction studies were carried out for **11** and the molecular structure is depicted in Figure 3, respectively. Selected bond lengths and angles are collected in Table 1, and the crystallographic details are reported in Table S3 in the SI. The molecular structure of **11** consists of a monomeric arrangement in the solid state. The zinc metal exhibits a distorted tetrahedral geometry, in which the pyrazolic nitrogens N(1) and N(3) occupy two positions and the acetamidinate nitrogen N(5) and the methyl carbon C(27) atoms occupy the other two positions. The distortion is due to the scorpionate ligand, which acts in a κ^3-NNN' coordination mode. The N(1)–Zn and N(3)–Zn bond lengths [2.068(6)

Å and 2.121(5) Å] compare well with that observed in the analogous acetamidinate-based scorpionate zinc alkyls,[25] but are considerably longer than the N(5)–Zn bond length [2.017(5) Å]. The solid-state structure also confirms that the acetamidinate is coordinated in a monodentate fashion to the Zn atom, and delocalization is also evidenced in the N–C–N moiety of the acetamidinate, with the bond lengths C(12)–N(5) and C(12)–N(6) ranging from 1.361(8) Å to 1.298(8) Å. Finally, the Zn–C(27) bond length [1.953(8) Å] can be regarded as normal considering the distances reported for analogs zinc alkyls.[25]

Figure 3. ORTEP view of [Zn(Me)(κ^3-phbpamd)] (**11**). Hydrogen atoms have been omitted for clarity. Thermal ellipsoids are drawn at the 30% probability level.

Table 1. Bond lengths [Å] and angles [°] for **1**, **7** and **11**.

1		7		11	
Distance (Å)					
Al(1)-N(5)	1.9439(19)	Al(1)-C(19)	1.958(3)	Zn(1)-N(1)	2.121(5)
Al(1)-N(6)	1.945(2)	Al(1)-C(20)	1.959(3)	Zn(1)-N(3)	2.068(6)
Al(1)-C(31)	1.968(3)	Al(1)-N(1)	1.963(2)	Zn(1)-N(5)	2.017(5)
Al(1)-C(32)	1.972(3)	Al(1)-N(5)	1.862(2)	Zn(1)-C(27)	1.953(8)
N(5)-C(24)	1.337(3)	N(5)-C(12)	1.357(3)	C(12)-N(5)	1.361(8)
N(6)-C(24)	1.330(3)	N(6)-C(12)	1.398(3)	C(12)-N(6)	1.298(8)
C(23)-C(24)	1.544(3)	C(11)-C(12)	1.361(3)	C(11)-C(12)	1.565(10)
Angles(º)					
N(5)-Al(1)-N(6)	68.75(8)	N(5)-Al(1)-C(19)	115.7(1)	C(27)-Zn(1)-N(5)	131.5(3)
N(5)-Al(1)-C(31)	114.45(10)	N(5)-Al(1)-C(20)	111.7(1)	C(27)-Zn(1)-N(3)	124.4(3)
N(6)-Al(1)-C(31)	116.61(11)	C(19)-Al(1)-C(20)	115.2(1)	N(5)-Zn(1)-N(3)	89.6(2)
N(5)-Al(1)-C(32)	113.59(10)	N(5)-Al(1)-N(1)	94.23(8)	C(27)-Zn(1)-N(1)	122.2(2)
N(6)-Al(1)-C(32)	111.35(10)	C(19)-Al(1)-N(1)	106.4(1)	N(5)-Zn(1)-N(1)	89.0(2)
C(31)-Al(1)-C(32)	120.95(12)	C(20)-Al(1)-N(1)	111.4(1)	N(3)-Zn(1)-N(1)	87.5(2)
C(24)-N(5)-C(28)	127.08(18)	C(12)-N(5)-C(13)	118.0(2)	C(12)-N(5)-C(13)	122.1(6)
C(24)-N(5)-Al(1)	89.89(13)	C(12)-N(5)-Al(1)	118.19(14)	C(12)-N(5)-Zn(1)	119.7(4)
C(28)-N(5)-Al(1)	142.42(15)	C(13)-N(5)-Al(1)	123.61(15)	C(13)-N(5)-Zn(1)	118.2(4)
C(24)-N(6)-C(25)	131.26(19)	C(12)-N(6)-C(15)	121.09(16)	C(12)-N(6)-C(20)	122.8(6)
C(24)-N(6)-Al(1)	90.02(14)	C(12)-C(11)-N(4)	123.34(19)	N(4)-C(11)-N(2)	109.8(5)
C(25)-N(6)-Al(1)	137.34(15)	C(12)-C(11)-N(2)	123.1(2)	N(4)-C(11)-C(12)	114.7(5)
N(6)-C(24)-N(5)	110.89(19)	N(4)-C(11)-N(2)	113.51(16)	N(2)-C(11)-C(12)	110.0(5)
N(6)-C(24)-C(23)	129.2(2)	C(11)-C(12)-N(5)	121.21(19)	N(6)-C(12)-N(5)	125.7(6)

N(5)-C(24)-C(23)	119.80(19)	C(11)-C(12)-N(6)	117.98(19)	N(6)-C(12)-C(11)	120.4(6)
		N(5)-C(12)-N(6)	120.77(18)	N(5)-C(12)-C(11)	113.6(6)

DFT Calculations

Density Functional Theory (DFT) calculations[31] were carried out to gain more insight into the (i) the influence of the bulkiness of the ligand on the observed coordination modes, (ii) the different thermodynamic stability of the tautomers C−H and N−H, and (iii) gain more insight into the Al-to-Zn ligand exchange processes.

To this end, we first explored the different coordination modes of species **7**, [Al(Me)$_2$(κ^2-tbpamd)], bearing the low sterically hindered acetamidinate-based tbpamd ligand. Our calculations indicate that the most thermodynamically stable species is the corresponding acetamidinate monodentate tautomer N−H, which lies 6.9 kcal/mol below the acetamidinate bidentate species (see Figure 4). This result is therefore fully consistent with the experimental solid-state findings (see above). In addition, the tautomer N−H is also 4.7 kcal/mol more stable than the corresponding C−H tautomer, which is consistent with the C−H to N−H isomerization observed for this complex in the NMR experiments (vide supra).[32]
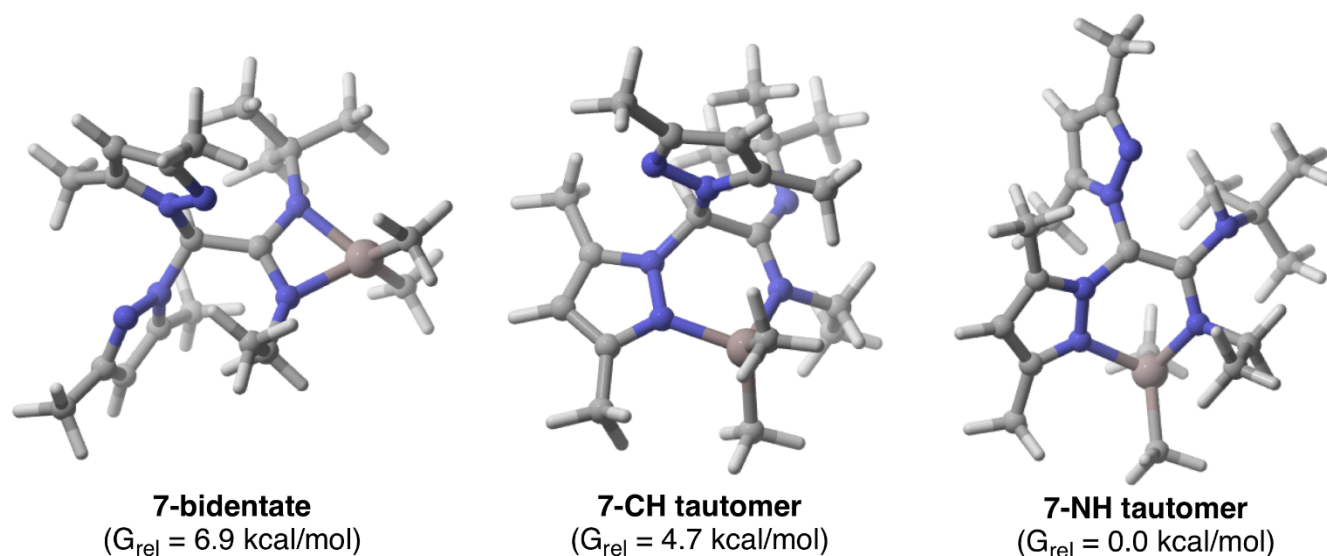

| **7-bidentate** | **7-CH tautomer** | **7-NH tautomer** |
| (G_{rel} = 6.9 kcal/mol) | (G_{rel} = 4.7 kcal/mol) | (G_{rel} = 0.0 kcal/mol) |

Figure 4. Fully optimized geometries and relative free energies (in kcal/mol) of the possible isomers for species **7** (R^1 = Et, R^2 = ^{t}Bu, see Scheme 1). Data computed at the PCM-B3LYP-D3/6-31G(d) level.

Similar results were found for species **8**, [Al(Me)$_2$(κ^2-phbpamd)], containing the related phbpamd ligand. Thus, the N−H tautomer lies 3.3 kcal/mol below the corresponding bidentate complex. In this

particular case, the C−H tautomer is energetically degenerate to its N−H counterpart, which nicely matches the 1:1 tautomers ratio found in the ^{1}H-NMR spectra. In sharp contrast, when considering a high sterically hindered ligand such as pbp^{t}amd in species **1**, [Al(Me)$_2$(κ^2-pbp^{t}amd)], the corresponding bidentate coordination mode is strongly favored as the corresponding C−H tautomer lies 12.3 kcal/mol above the bidentate species. This remarkable destabilization of the acetamidinate monodentate species may be ascribed to the unfavorable steric interaction between the bulky ^{t}Bu and ^{i}Pr groups which is not present in the species having methyl substituted pyrazole rings. This result is once again fully consistent with the experimental findings and can be extrapolated to other sterically encumbered ligands (tbp^{t}amd or phbp^{t}amd) and provides further support to the selected computational method for this study.

We then considered the ligand exchange process which leads to the formation of the complexes [Zn(Me)(κ^3-NNN')] (**10–11**). To this end, we explored the reaction of species **8** (from its C−H tautomer) with ZnMe$_2$ which lead to **11**. Our calculation indicates that the ligand exchange process is thermodynamically favored as the reaction is exergonic ($\Delta G_R = -3.4$ kcal/mol). Although the reaction mechanism involved in this transmetalation process is however not clear at this moment, the computed exergonicity and the fact that the transformation occurs at 20 ºC suggest that the associated activation barrier should be relatively low.

Polymerization Studies.

The main aim of these studies was to compare the activity and stereoselectivity of both families of mononuclear initiators, namely the high sterically hindered acetamidinate bidentate dialkyls **1−6** and the low sterically demanded acetamidinate monodentate dialkyls **7−9** species. Finally, it was also our intention to establish a comparison with analog scorpionate aluminum dialkyls, and other remarkable organo-aluminum initiators reported to date.

Thus, complexes **1**, **5**, **7** and **8** were systematically evaluated in the ring-opening polymerization (ROP) of the polar monomer ε-caprolactone (ε-CL) and *rac*-lactide (*rac*-LA) at 50ºC and 70ºC in toluene as solvent under a nitrogen atmosphere for the production of poly(ε-caprolactone)s (PCLs) (see Table S2) and poly(*rac*-lactide)s (PLAs) (see Table 2), respectively. The reactions were initially carried out both without the need for an activator and, alternatively, under the presence of different molar ratios of BnOH as cocatalyst. The experimental medium-low M_n values of the PCLs and PLAs produced were determined by size exclusion chromatography (SEC) using the respective Mark–Houwink corrections,[33] and showed to be in close agreement with the expected theoretical calculated values considering one polymer chain per aluminum center for both cyclic polar monomers (see Table S2 and Table 2). In addition, analysis of the resulting polyesters revealed a monomodal weight distribution, with narrow dispersity values ranging from 1.08 to 1.17 (see Figure S10 in the SI).

Initiators were assessed in the polymerization of CL employing 300 equiv. of monomer at 50ºC to demonstrate their catalytic activity (see Table S2). It was found that the nature of the substituents in the pyrazole rings has a significant effect on the catalytic activity (ᵗBu > Me), with almost complete conversion in 10 hours. It is worth noting that these activity values are much higher than those reported for analogs based on acetamidate- and thioacetamidate-based heteroscorpionate[17] and mononuclear phenolato[28d] aluminum initiators in the polymerization of this monomer. Indeed, no polymerization activity was reported at 50ºC for these species which, in addition, require more severe conditions, and much longer reaction times to obtain comparable conversions (see Table S2). However, initiators **1**, **5**, **7** and **8** resulted comparatively less active than alternative N,N,O-chelate aluminum complexes[34] (50ºC, 120 min, 95%

conv.).

Furthermore, **1**, **5**, **7** and **8** were systematically examined for the production of poly(*rac*-lactide) (PLA), and it was found that they behaved as active single-component living catalysts and polymerized 200 equivalents of *rac*-LA at 70 ºC in 18 hours under identical conditions (see Table 2), to provide narrow monomodal molecular weight distributions.

In particular, complex **1** transformed 81% of the monomer after 18 hours at 70 ºC, while **5** produces 96% of polymer under identical conditions (entries 1 and 2, respectively), probably due to the presence of more sterically hindered phenyl substituents in the acetamidinate fragment, which suppress more efficiently at that temperature the possible formation of the previously reported homoleptic sandwich-like bis(scorpionate)aluminum monoalkyl species[17b] that disfavor catalytic performance.

Moreover, the N−H tautomer initiator **7** resulted less active than the mixture of C−H and N−H tautomers in **8**, with the 75% and 85%, respectively, of the monomer transformed as a result of the additional higher steric hindrance of the phenyl substituents in the ligand (entries 11 and 12). Nonetheless, **7** and **8** showed levels of material production lower than that found for the higher sterically hindered counterpart **5**.

In similar way to the CL monomer, all these initiators offered activities in the ROP of *rac*-LA higher than acetamidate- and thioacetamidate-based scorpionate aluminum analogs described previously in our group (70ºC and 72h[17a] (entry 15) or 110ºC and 6-16 h,[17b] to reach complete conversion) and organoaluminum supported by 6,6'-dimethylbiphenyl-bridged salen ligands (110ºC and 60-132 h to reach complete conversion),[35] and N,N,O-chelate aluminum complexes,[34] which require harsher conditions or simply resulted inactive. In addition, the activity of these initiators paralleled those reported employing alkyl aluminum complexes supported by salicylbenzoxazole (70ºC, 8-108 h)[23a] and bis(pyrrolidene) schiff base (70ºC, 12-144 h)[23c] ligands, although they are less active than a recently reported C_2-symmetric salen aluminum initiator,[36] very efficient at room temperature.

The effect of solvent and temperature was also examined. Thus, all initiators maintained significant catalytic conversions even at 50 ºC, with only a slight reduction in the dispersity values (Table 2, entries

5 and 13). In addition, a significant reduction in catalytic performance was observed on using tetrahydrofuran (Table 2, entry 4), as a result of the possible competence of this solvent with the aluminum center for the lactide monomer.

The good level of control afforded by these initiators in the ROP of these monomers was further exemplified by initiator **5**, which gave rise to linear correlations between M_n and percentage conversion (see Figure S11 in the SI, $R^2 = 0.991$) in conjunction with narrow molecular weight distributions. Also, a double-feed experiment resulted in a polymer chain extension with analogs polymer features, confirming the well-controlled living performance of catalyst **5** (entries 2 and 3) and the existence of a single type of reaction site.

In order to acquire better initiation efficiencies and well-controlled polymerization procedures, initiators **5** and **8** were also performed under "*immortal*" conditions,[23a,33,37] in which excess of benzyl alcohol molecules were added, acting as a chain transfer agent (CTA). Thus, we initially added three equivalents of benzyl alcohol (Table 2, entries 6 and 14), and all initiators could catalyze the ROP of *rac*-LA to PLAs with the observed molecular weights close to the theoretical values corrected by the equiv. of benzyl alcohol added, and the narrow dispersities, evidencing the living and immortal character of the reaction. The immortal character of **5** was also inspected by increasing the ratio of [Al] : [*rac*-LA]$_0$: [PhCH$_2$OH] from 1 :200 : 3 to 1 :1000 : 10 (Table 2, entries 6−10). As expected, a decreased in the M_n of the resulting polymers proportional to the monomer/benzyl alcohol ratio was observed, with molecular weight distributions still narrow. These results indicate that in the presence of excess benzyl alcohol molecules undesired ligand dissociation does not occur during the reaction, and suggest that a fast-reversible exchange between dormant hydroxyl-end-capped polymer chains/free PhCH$_2$OH and the active Al-alkoxy type polymer chain, significantly faster than the chain propagation, takes place instead.[23a,35] Consequently, the ROP of *rac*-LA mediated by initiators **5** and **8** under immortal conditions is an effective method for the synthesis of low molecular weight PLAs using only a small amount of catalyst.

In addition, low molecular weight materials produced by initiator **5** were examined by MALDI−ToF MS (see Figures S12a and b in the SI), and end-group analyses by ^{1}H NMR of poly(*rac*-

lactide) oligomers were also inspected (see Figures S13a and b in the SI). These two outcomes provide evidence that the ring-opening of *rac*-LA occurs by the initial addition of the alkyl/BnO fragment to the monomer in the produced materials, with cleavage of the acyl-oxygen bond[38] followed by further monomer additions to the (macro)alcohols.

Table 2. Polymerization of *rac*-Lactide Catalyzed by Complexes 1, 5, 7 and 8[a]

entry	initiator	$[Al]_0$:$[rac$-LA$]_0$:$[BnOH]$	temp (°C)	time (h)	yield (g)	conv (%)[b]	$M_{n(theor.)}$ (Da)[c]	M_n (Da)[d]	M_w/M_n[d]	P_s[e]
1	**1**	1:200:0	70	18	2.10	81	23 300	24 400	1.11	0.61
2	**5**	1:200:0	70	18	2.49	96	27 700	26 800	1.09	0.65
3	**5**	1:200:0	70	36	5.03	97	56 000	54 200	1.15	0.65
4	**5**[f]	1:200:0	70	18	1.50	58	16 700	17 300	1.12	0.64
5	**5**	1:200:0	50	18	1.27	49	14 100	13 200	1.08	0.70
6	**5**[g]	1:200:3	70	8	2.46	95	9 200	10 000	1.10	0.67
7	**5**[g]	1:200:10	70	6	2.49	96	2 900	3 500	1.11	0.65
8	**5**[g]	1:200:20	70	4	2.54	98	1 500	2 400	1.09	0.66
9	**5**[g]	1:500:10	70	6	1.09	84	6 100	5 500	1.11	0.63
10	**5**[g]	1:1000:10	70	6	1.87	72	10 500	9 300	1.12	0.62
11	**7**	1:200:0	70	18	1.94	75	21 600	25 100	1.14	0.63
12	**8**	1:200:0	70	18	2.20	85	24 500	25 600	1.15	0.63
13	**8**	1:200:0	50	18	1.22	47	13 500	14 400	1.14	0.65
14	**8**[g]	1:200:3	70	8	2.12	82	8 000	7 000	1.13	0.63
15	**[Al(Et)$_2$\{κ^2-(S)-mtbpam\}][h]**	1:200:0	70	72	1.04	40	11 520	11 140	1.04	0.60

[a] Polymerization conditions: (a) 90 μmol of initiator, $[rac$-LA$]_0$/$[Al]_0$ = 200 and 30 mL of toluene as solvent. [b] Percentage conversion of the monomer [(weight of polymer recovered/weight of monomer) × 100]. [c] Theoretical M_n = (monomer/initiator) × (% conversion) × (M_w of lactide). In addition to the cocatalyst BnOH, the theoretical M_n was calculated as [(monomer/initiator) × (% conversion/cocatalyst) × (M_w of lactide)] + M_w of BnOH. [d] Determined by GPC relative to polystyrene standards in tetrahydrofuran. Experimental M_n was calculated considering Mark–Houwink's corrections[33] for M_n [M_n(obsd.) = 0.58 × M_n(GPC)]. [e] P_s is the probability of racemic linkages between monomer units and is determined from the relative intensity

in the tetrads obtained in the decoupled ^{1}H NMR by $P_s = 2I_1/(I_1+I_2)$, with $I_1 = \delta$ 5.20–5.25 ppm (*sis*, *sii/iis*) and $I_2 = \delta$ 5.13–5.20 ppm (*iis/sii*, *iii*, *isi*).[39] [f] 10 mL of tetrahydrofuran as solvent. [g] Addition of BnOH as cocatalyst at several molar ratios. [h] These data have been included for comparison in ROP with acetamidate- and thioacetamidate-based heteroscorpionate aluminum dialkyl analogs.[17a]

Poly(*rac*-lactide) Microstructure Analysis. ^{1}H NMR microstructure analysis in the poly(*rac*-lactide)s produced by **1**, **5**, **7** and **8** in toluene have been carried out. For instance, **5** offers a modest level in the heterotactic dyad enchainment at 70 ºC (P_s = 0.65, Table 2, entry 2), which is also slightly higher than the low value found for **1** (P_s = 0.61, Table 2, entry 1). This can be attributed to the more sterically demanding environment produced by the the phenyl substituents in the phbp^{t}amd ligand, while the low sterically hindered acetamidinate bidentate aluminum dialkyls **7** and **8** exert from low to modest levels of heteroselectivity on the growing polymer microstructures (P_s = 0.63–0.65, Table 2, entries 11–14). In addition, immortal conditions did not reduce significantly the P_s values. More interestingly, a decrease of the temperature reaction at 50 ºC revealed an important increase on the hetero-activity imparted by **5**, reaching a P_s value up to 0.70 (Table 2, entry 5, see Figure S14 in the SI), probably through a chain end control mechanism.[40]

These findings clearly represent an interesting step forward on the employment of the scorpionate aluminum initiators in the ROP for *rac*-lactide, since high[17a] and low[17b-d] sterically hindered acetamidate- and thioacetamidate-based heteroscorpionate aluminum analogs reported in our group produced amorphous atactic poly(*rac*-lactide) materials (Table 2, entry 15). It is also worth mentioning that although the heteroselectivity values observed for the catalyst **5** are slightly lower than those reported to date for heteroselective aluminum initiators, such as that employing N,O-aminophenol based complexes[19a], or chiral anilido-oxazolinate complexes[19b] with (P_s = 0.74),[19] and much lower than that using salan–aluminum catalysts (P_s = 0.98)[20], these initiators resulted more heteroselective than that reported employing monomethylaluminum pyrrolylaldiminates (P_s = 0.60).[41]

CONCLUSIONS

In conclusion, we report herein the preparation of two new families of mononuclear aluminum dialkyls supported by bi- and monodentate acetamidinates with different steric congestion of the type [AlR$_2$(κ^2-N'N')] and [AlR$_2$(κ^2-NN')], respectively. In the acetamidinate monodentate derivatives, two possible CH−NH tautomers as low extended π-N−C−N'(sp^2)−Al and large extended π-HN−C$_2$−N'(sp^2)−Al complexes, respectively, could be identified. One tautomer can be efficiently converted into the other form throughout an apical C−H methine scorpionate activation, which resulted to be time dependent. In addition, aluminum dialkyls **7** and **8** when reacted with ZnMe$_2$ provided a very unusual ligand exchange process, which also involves zinc-to-aluminum transmetalation alkyl groups, to afford more stable scorpionate zinc monoalkyls [Zn(Me)(κ^3-NNN')]. Extensive X-ray diffraction analysis for **1**, **3**, the N–H tautomers of **7** and **8**, as well as **11** unambiguously confirmed the arrangements proposed in all families of compounds. Moreover, DFT calculations allowed us to gain more insight into the relative thermodynamical stabilities of the two different κ^2-arrangements found in both families of acetamidinate complexes, and for the two possible CH–NH tautomers, as well as for the κ^3-scorpionate zinc monoalkyls *versus* the κ^2-acetamidinate aluminum dialkyls.

Importantly, the dialkyls **1**, **5**, **7** and **8** can act as efficient single-component initiators for the living and immortal ROP of ε-CL and *rac*-LA in mild conditions after hours, as showed by the narrow dispersity values, as well as the good agreement between the experimental M_n values and monomer/benzyl alcohol ratios. Additionally, the highest sterically congested initiator **5** produced hetero-enriched poly(*rac*-lactide)s (P_s = 0.70).

Acknowledgments

Supporting Information Available: Details of Experimental section, ^{1}H NMR spectra for complexes **1**, **7**, **8** and **9**, VT ^{1}H NMR experiments of **9**, X-ray diffraction studies of the protioligand **b x 0.5C$_4$H$_8$O**, **3** and **8**, and ring-opening polymerization of ε-caprolactone and *rac*-lactide. X-ray diffraction experimental details for the protioligand **b x 0.5C$_4$H$_8$O** and the complexes **1**, **3**, **7**, **8 x 0.5C$_6$H$_{14}$**, and **11**, and DFT calculations experimental details are also included. This material is available free of charge via the Internet at http://pubs.acs.org.

References

(1)   For reviews in this area see: (*a*) Galbis, J. A.; García-Martín, M. d. G.; de Paz, V.; Galbis, E. Synthetic Polymers from Sugar-Based Monomers. *Chem. Rev.* **2016**, *116*, 1600–1636; (*b*) Guillaume, S. M.; Kirillov, E.; Sarazin, Y.; Carpentier, J.-F. Beyond Stereoselectivity, Switchable Catalysis: Some of the Last Frontier Challenges in Ring-Opening Polymerization of Cyclic Esters. *Chem. – Eur. J.* **2015**, *21*, 7988–8003. (*c*) Cameron, D. J. A.; Shaver, M. P. Aliphatic Polyester Polymer Stars: Synthesis, Properties and Applications in Biomedicine and Nanotechnology. *Chem. Soc. Rev.* **2011**, *40*, 1761–1776.

2)   For books in this area see: (*a*) Jiménez, A.; Peltzer, M.; Ruseckaite, R. *Poly(lactic acid) Science and Technology : Processing, Properties, Additives and Applications*. RSC Polymer Chemistry Series, 2014. (*b*) Auras, R.; Lim, L.-T. *Poly(lactic Acid) : Synthesis, Structures, Properties, Processing, and Applications*. Wiley: Hoboken, NJ, 2010. (*c*) Dubois, P.; Coulembier, O.; Raquez, J.-M. *Handbook of Ring-Opening Polymerization*. Wiley-VCH: Weinheim, 2009.

(3)   Ragauskas, A. J.; Williams, C. K.; Davison, B. H.; Britovsek, G.; Cairney, J.; Eckert, C. A.; Frederick, W. J., Jr.; Hallett, J. P.; Leak, D. J.; Liotta, C. L.; Mielenz, J. R.; Murphy, R.; Templer, R.; Tschaplinski, T. The Path Forward for Biofuels and Biomaterials. *Science* **2006**, *311*, 484–489.

(4)   *Institute for Bioplastics and Biocomposites*: Biopolymers – facts and statistics, edition 2017. Hanover, Germany, 2017. (https://www.ifbb-hannover.de/de/facts-and-statistics.html).

(5)   Pêgo, A. P.; Siebum, B.; Van Luyn, M. J.; Gallego y Van Seijen, X. J.; Poot, A. A.; Grijpma, D. W.; Feijen J. Preparation of Degradable Porous Structures Based on 1,3-Trimethylene Carbonate and D,L-Lactide (Co)polymers for Heart Tissue Engineering. *Tissue Eng. Pt. A* **2003**, *9*, 981–994.

(6)   Tyler, B.; Gullotti, D.; Mangraviti, A.; Utsuki, T.; Brem, H. Polylactic acid (PLA) controlled delivery carriers for biomedical applications. *Adv. Drug Deliv. Rev.* **2016**, 107, 163–175.

(7)   (*a*) Inkinen, S.; Hakkarainen, M.; Albertsson, A.-C.; Södergård, A. From Lactic Acid to Poly(lactic acid) (PLA): Characterization and Analysis of PLA and Its Precursors. *Biomacromolecules* **2011**, *12*, 523–532. (*b*) Darensbourg, D. J.; Choi, W.; Richers, C. P. Ring-Opening Polymerization of Cyclic Monomers by Biocompatible Metal Complexes. Production of Poly(lactide), Polycarbonates, and Their Copolymers. *Macromolecules* **2007**, *40*, 3521–3523.

(8)   (*a*) Parkin, G. The Bioinorganic Chemistry of Zinc: Synthetic Analogues of Zinc Enzymes That Feature Tripodal Ligands. *Chem. Commun.* **2000**, 1971–1985. (*b*) Mills, C. F. *Zinc in Human Biology*, Springer-Verlag, New York, 1989.

(9)   (*a*) Cowan, J. A. Ed. *The Biological Chemistry of Magnesium*; VCH: New York, 1995. (*b*) Campbell, N. A. *Biology*, 3rd ed.; Benjamin/Cummings Publishing Company: Redwood City, CA, 1993; pp 718 and 811.

(10)   Carpentier J.-F., Sarazin, Y. *Alkaline-Earth Metal Compounds: Oddities and Applications,* Springer Berlin Heidelberg, Berlin, 2013, pp: 141-189.

(11)   Wei, Y.; Wang, S.; Zhou, S.; Aluminum Alkyl Complexes: Synthesis, Structure, and Application in ROP of Cyclic Esters. *Dalton Trans*. **2016**, *45*, 4471–4485.

(12)   (*a*) Le Roux, E. Recent Advances on Tailor-Made Titanium Catalysts for Biopolymer Synthesis. *Coord. Chem. Rev*. **2016**, *306*(Part 1), 65–85.

(13)   (*a*) Aluthge, D. C.; Ahn, J.-M., Mehrkhodavandi, P. Overcoming Aggregation in Indium Salen Catalysts for Isoselective Lactide Polymerization. *Chem. Sci.* **2015**, 6, 5284–5292. (*b*) Horeglad, P.; Szczepaniak, G.; Dranka, M.; Zachara, J. The First Facile Stereoselectivity Switch in the Polymerization of rac-Lactide-From Heteroselective To Isoselective Dialkylgallium Alkoxides with the Help of N-Heterocyclic Carbenes. *Chem. Commun.* **2012**, *48*, 1171–1173.

(14)   (*a*) Bakewell, C.; White, A. J. P.; Long, N.; Williams, C. K. Metal-Size Influence in Iso-Selective Lactide Polymerization. *Angew. Chem., Int. Ed.* **2014**, *53*, 9226–9230. (*b*) Bakewell, C.; Cao, T.-P.-A.; Long, N.; Le Goff, X. F.; Auffrant, A. Williams, C. K. Yttrium Phosphasalen Initiators for rac-Lactide Polymerization: Excellent Rates and High Iso-Selectivities. *J. Am. Chem. Soc.* **2012**, *134*, 20577–20580.

(15)   (*a*) Honrado, M.; Otero, A.; Fernández-Baeza, J.; Sánchez-Barba, L. F.; Garcés, A.; Lara-Sánchez. A.; Rodríguez, A. M. Copolymerization of Cyclic Esters Controlled by Chiral NNO-Scorpionate Zinc Initiators. *Organometallics* **2016**, *35*, 189–197. (*b*) Honrado, M.; Otero, A.; Fernández-Baeza, J.; Sánchez-Barba, L. F.; Garcés, A.; Lara-Sánchez, A.; Martínez-Ferrer, J.; Sobrino, S.; Rodríguez, A. M. New Racemic and Single Enantiopure Hybrid Scorpionate/Cyclopentadienyl Magnesium and Zinc Initiators for the Stereoselective ROP of Lactides. *Organometallics* **2015**, *34*, 3196−3208.

(16)   (*a*) Garcés, A.; Sánchez-Barba, L. F.; Fernández-Baeza, J.; Otero, A.; Lara-Sánchez, A.; Rodríguez, A. M. Studies on Multinuclear Magnesium *tert*-Butyl Heteroscorpionates: Synthesis, Coordination Ability, and Heteroselective Ring-Opening Polymerization of rac-Lactide. *Organometallics* **2017**, *36*, 884−897. (*b*) Garcés, A.; Sánchez-Barba, L. F.; Fernández-Baeza, J.; Otero, A.; Honrado, M.; Lara-Sánchez, A.; Rodríguez, A. M. Heteroscorpionate Magnesium Alkyls Bearing Unprecedented Apical σ-C(sp^3)–Mg Bonds: Heteroselective Ring-Opening Polymerization of rac-Lactide. *Inorg. Chem*. **2013**, *52*, 12691−12701.

(17)   (*a*) Castro-Osma, J. A.; Alonso-Moreno, C.; Lara-Sánchez, A.; Otero, A.; Fernández-Baeza, J.; Sánchez-Barba, L. F.; Rodríguez, A. M. Catalytic Behaviour in the Ring-Opening Polymerisation of Organoaluminiums Supported by Bulky Heteroscorpionate Ligands. *Dalton Trans*. **2015**, *44*, 12388–12400. (*b*) Castro-Osma, J. A.; Alonso-Moreno, C.; Otero, A.; Lara-Sánchez, A.; Fernández-Baeza, J.; Rodríguez, A. M.; Sánchez-Barba, L. F.; García-Martínez, J. C. Synthesis, Structural Characterization and Catalytic Evaluation of the Ring-Opening Polymerization of Discrete Five-Coordinate Alkyl Aluminium Complexes. *Dalton Trans*. **2013**, *42*, 9325–9337.

(18)   Otero, A.; Fernández-Baeza, J.; Lara-Sánchez, A.; Sánchez-Barba, L. F. Metal Complexes with Heteroscorpionate Ligands Based on the Bis(pyrazol-1-yl)methane Moiety: Catalytic Chemistry. *Coord. Chem. Rev.* **2013**, *257*, 1806–1868.

(19)   (*a*) Roymuhury, S. K.; Chakraborty, D.; Ramkumar, V. Aluminium Complexes Bearing N,O-Aminophenol Ligands as Efficient Catalysts for the Ring Opening Polymerization of Lactide. *Eur. Polym. J.* **2015**, *70*, 203–214. (*b*) Bian, S.; Abbina, S.; Lu, Z.; Kolodka, E.; Du, G. Ring-Opening Polymerization of rac-Lactide with Aluminum Chiral Anilido-Oxazolinate Complexes. *Organometallics* **2014**, *33*, 2489−2495.

(20)   Press, K.; Goldberg, I., Kol., M. Mechanistic Insight into the Stereochemical Control of Lactide Polymerization by Salan–Aluminum Catalysts. *Angew. Chem. Int. Ed.* **2015**, *54*, 14858–14861.

(21) Chen, H-L.; Dutta, S.; Huang, P-Y.; Lin, C-C. Preparation and Characterization of Aluminum Alkoxides Coordinated on Salen-Type Ligands: Highly Stereoselective Ring-Opening Polymerization of rac-Lactide. *Organometallics* **2012**, *31*, 2016–2025.

(22) Bakewell, C.; Platel, R. H.; Cary, S. K.; Hubbard, S. M.; Roaf, J. M.; Levine, A. C.; White, A. J. P.; Long, N. J.; Haaf, M.; Williams, C. K. Bis(8-quinolinolato)aluminum Ethyl Complexes: Iso-Selective Initiators for rac-Lactide Polymerization. *Organometallics* **2012**, *31*, 4729−4736.

(23) (*a*) Sumrit, P.; Chuawong, P.; Nanok, T.; Duangthongyou, T.; Hormnirun, P. Aluminum Complexes Containing Salicylbenzoxazole Ligands and Their Application in the Ring-Opening Polymerization of rac-Lactide and ε-Caprolactone. *Dalton Trans*. **2016**, *45*, 9250–9266. (*b*) Nakonkhet, C.; Nanok, T.; Wattanathana, W.; Chuawong, P.; Hormnirun, P. Aluminium Complexes Containing Salicylbenzothiazole Ligands and Their Application in the Ring-Opening Polymerisation of rac-Lactide and ε-Caprolactone. *Dalton Trans*. **2017**, 46, 11013–11030. (*c*) Tabthong, S.; Nanok, T.; Sumrit, P.; Kongsaeree, P.; Prabpai, S.; Chuawong, P.; Hormnirun, P. Bis(pyrrolidene) Schiff Base Aluminum Complexes as Isoselective-Biased Initiators for the Controlled Ring-Opening Polymerization of rac-Lactide: Experimental and Theoretical Studies. *Macromolecules* **2015**, *48*, 6846−6861. (*d*) McKeown, P.; Davidson, M. G.; Kociok-Köhnb, G.; Jones, M. D. Aluminium Salalens vs. Salans: "Initiator Design" for the Isoselective Polymerisation of rac-Lactide. *Chem. Commun*. **2016**, 52, 10431−10434.

(24) Shen, M.; Zhang, W.; Nomura, K.; Sun, W.-H. Synthesis and Characterization of Organoaluminum Compounds Containing Quinolin-8-Amine Derivatives and Their Catalytic Behaviour for Ring-Opening Polymerization of ε-Caprolactone. *Dalton Trans*. **2009**, 9000–9009.

(25) Alonso-Moreno, C.; Garcés, A.; Sánchez-Barba, L. F.; Fajardo, M.; Fernández-Baeza, J.; Otero, A.; Antiñolo, A.; Lara-Sánchez, A.; Broomfield, L.; López-Solera, I.; Rodríguez, A. M.

Discrete Heteroscorpionate Lithium and Zinc Alkyl Complexes. Synthesis, Structural Studies, and ROP of Cyclic Esters. *Organometallics* **2008**, *27*, 1310–1321.

(26)   Abeysekera, D.; Robertson, K. N.; Cameron, T. S.; Clyburne, J. A. C. m-Terphenyl-Substituted Amidinates: Useful Ligands in the Preparation of Robust Aluminum Alkyls. *Organometallics* **2001,** *20,* 5532–5536.

(27)   (*a*) Gutschank, B.; Schulz, S.; Marcinkowski, M.; Jansen, G.; Bandmann, H.; Bläser, D.; Wölper, C. Synthesis, Structure, Tautomerism, and Reactivity of Methanetrisamidines. *Angew. Chem. Int. Ed.* **2012**, *51*, 10893 –10897. (*b*) Gutschank, B.; Schulz, S.; Bläser, D.; Wölper, C. Methanetrisamidines in Coordination Chemistry - Syntheses, Structures and CH-NH Tautomerism. *Dalton Trans*. **2014**, 43, 2907–2914. (*c*) Gutschank, B.; Bayram, M.; Schulz, S.; Bläser, D.; Wölper, C. Heterobimetallic Metal–Amidinate Complexes by Stepwise Metalation of Methanetrisamidines. *Eur. J. Inorg. Chem.* **2013**, 5495–5502.

(28)   (*a*) Isnard, F.; Lamberti, M.; Lettieri, L.; D'auria, I.; Press, K.; Troiano, R.; Mazzeo, M. Bimetallic Salen Aluminum Complexes: Cooperation Between Reactive Centers in the Ring-Opening Polymerization of Lactides and Epoxides. *Dalton Trans.* **2016**, *45*, 16001–16010. (*b*) Thevenon, A.; Romain, C.; Bennington, M. S.; White, A. J. P.; Davidson, H. J.; Brooker, S.; Williams, C. K. Polymerization Catalysts: Hyperactivity by Control of Ligand Conformation and Metallic Cooperativity. *Angew. Chem., Int. Ed.* **2016**, *55*, 8680–8685. (*c*) Otero, A.; Fernández-Baeza, J.; Sánchez-Barba, L. F.; Sobrino S.; Garcés, A.; Lara-Sanchez, A.; Rodriguez, A. M. Mono- and Binuclear Chiral N,N,O-Scorpionate Zinc Alkyls as Efficient Initiators for the ROP Of rac-Lactide. *Dalton Trans*. **2017**, *46*, 15107-15117. (*d*) Tseng, H.-C.; Chen, H.-Y.; Huang, Y.-T.; Lu, W.-Y.; Chang, Y.-L.; Chiang, M. Y.; Lai, Y.-C.; Chen, H.-Y. Improvement in Titanium Complexes Bearing Schiff Base Ligands in the Ring-Opening Polymerization of L-Lactide: A Dinuclear System with Hydrazine-Bridging Schiff Base Ligands. *Inorg. Chem.* **2016**, *55*, 1642–1650.

(29)   Garcés, A.; Sánchez-Barba, L. F.; Alonso-Moreno, C.; Fajardo, M.; Fernández-Baeza, J.; Otero, A.; Lara-Sánchez, A.; López-Solera, I.; Rodríguez, A. M. Hybrid Scorpionate/Cyclopentadienyl Magnesium and Zinc Complexes: Synthesis, Coordination Chemistry, and Ring-Opening Polymerization Studies on Cyclic Esters. *Inorg. Chem.* **2010**, *49*, 2859–2871.

(30)   Kaczorowski, T.; Justyniak, I.; Prochowicz, D.; Zelga, K.; Kornowicz, A.; Lewiński, J. New Insights into Cinchonine–Aluminium Complexes and Their Application as Chiral Building Blocks: Unprecedented Ligand-Exchange Processes in the Presence of ZnR_2 Compounds. *Chem. – Eur. J.* **2012**, *18*, 13460–13465.

(31)   See Computational Details in the Supporting Information.

(32)   For both tautomers, the possible isomers where the ethyl and *tert*-butyl groups are interchanged, i.e. R^1 = ^tBu and R^2 = Et (see Scheme 1) were also computed. Our calculations indicate that these alternative isomers are destabilized with respect to the experimentally observed (See X-ray studies) isomers [ΔG = 6.0 and 6.8 kcal/mol, for the C–H and N–H tautomers, respectively].

(33)   (*a*) Inoue, S. Immortal Polymerization: The Outset, Development, and Application. *J. Polym. Sci. Part a: Polym. Chem*. **2000**, *38*, 2861–2871. (*b*) Baran, J.; Duda, A.; Kowalski, A.; Szymanski, R.; Penczek, S. Intermolecular Chain Transfer to Polymer with Chain Scission: General Treatment and Determination of k_p/k_{tr} in L,L-Lactide Polymerization. *Macromol. Rapid Commun*. **1997**, *18*, 325–333.

(34)   Kong, W-L.; Chai, Z-Y.; Wang, Z-X. Synthesis of N,N,O-Chelate Zinc and Aluminum Complexes and Their Catalysis in the Ring-Opening Polymerization of ε-Caprolactone and rac-Lactide. *Dalton Trans*. **2014**, *43*, 14470−14480.
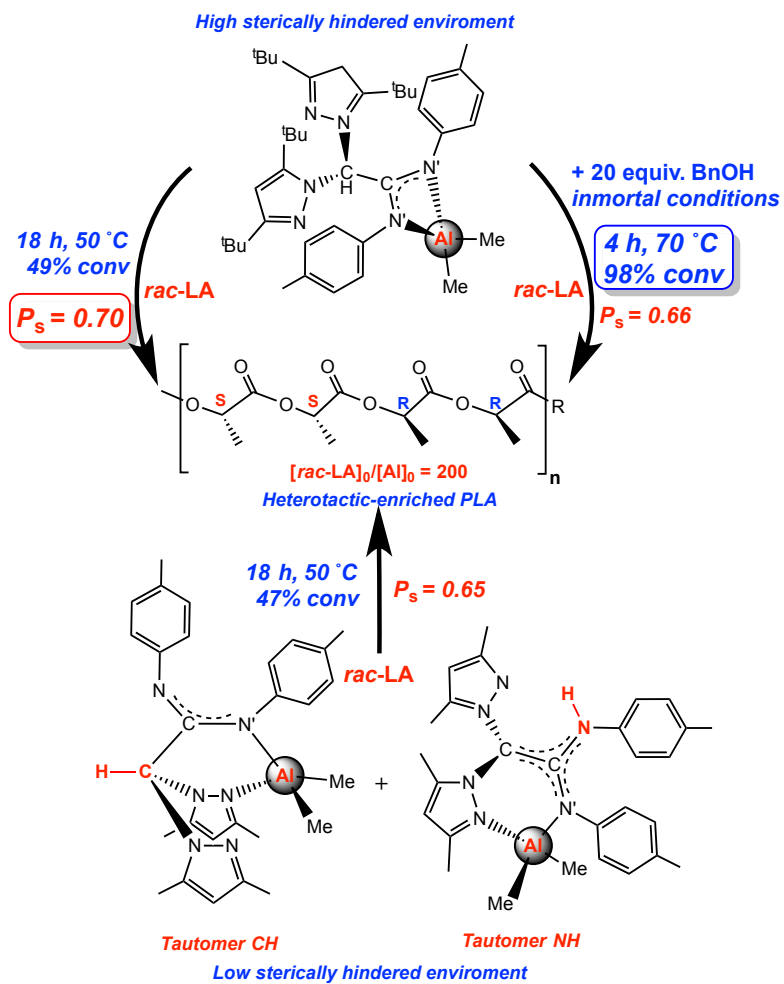
(35)   Kan, C.; Ge, J.;Ma, H. Aluminum Methyl, Alkoxide and α-Alkoxy Ester Complexes Supported by 6,6'-Dimethylbiphenyl-Bridged Salen Ligands: Synthesis, Characterization and Catalysis for rac-Lactide Polymerization. *Dalton Trans.* **2016**, *45*, 6682–6695.

(36)   Robert, C.; Schmid, T. E.; Richard, V.; Haquette, P.; Raman, S. K.; Rager, M.-N.; Gauvin, R. M.; Morin, Y.; Trivelli, X.; Guérineau, V.; del Rosal, I.; Maron, L.; Thomas, C. M. Mechanistic Aspects of the Polymerization of Lactide Using a Highly Efficient Aluminum(III) Catalytic System. *J. Am. Chem. Soc.* **2017**, *139*, 6217−6225.

(37)   (*a*) Normand, M.; Dorcet, V.; Kirillov, E.; Carpentier, J.-F. {Phenoxy-imine}aluminum versus Indium Complexes for the Immortal ROP of Lactide: Different Stereocontrol, Different Mechanisms. *Organometallics* **2013**, *32*, 1694–1709; (*b*) Hild, F.; Neehaul, N.; Bier, F.; Wirsum, M.; Gourlaouen, C.; Dagorne, S. Synthesis and Structural Characterization of Various N,O,N-Chelated Aluminum and Gallium Complexes for the Efficient ROP of Cyclic Esters and Carbonates: How Do Aluminum and Gallium Derivatives Compare?. *Organometallics* **2013**, *32*, 587–598.

(38)   Sánchez-Barba, L. F.; Hughes, D. L.; Humphrey, S. M.; Bochmann, M. Ligand Transfer Reactions of Mixed-Metal Lanthanide/Magnesium Allyl Complexes with β-Diketimines: Synthesis, Structures, and Ring-Opening Polymerization Catalysis. *Organometallics* **2006**, *25*, 1012−1020.

(39)   Drouin, F.; Oguadinma, P. O.; Whitehorne, T. J. J.; Prud'homme, R. E.; Schaper, F. Lactide Polymerization with Chiral β-Diketiminate Zinc Complexes. *Organometallics* **2010**, *29*, 2139−2147.

(40)   Nomura, N.; Ishii, R.; Yamamoto, Y.; Kondo, T. Stereoselective Ring-Opening Polymerization of a Racemic Lactide by Using Achiral Salen– and Homosalen–Aluminum Complexes. *Chem. - Eur. J.* **2007**, *13*, 4433−4451.

(41)   Tabthong, S.; Nanok, T.; Kongsaeree, P.; Prabpaib, S.; Hormnirun, P. Monomethylaluminum and Dimethylaluminum Pyrrolylaldiminates for the Ring-Opening Polymerization of rac-Lactide: Effects of Ligand Structure and Coordination Geometry. *Dalton Trans.* **2014**, *43*, 1348–1359.

Organo-Aluminum and Zinc Acetamidinates: Preparation, Coordination Ability and ROP Processes of Cyclic Esters

Andrés Garcés,[†] Luis F. Sánchez-Barba,[*,†] Juan Fernández-Baeza,[‡] Antonio Otero,[*,‡] Israel Fernández,[§] Agustín Lara-Sánchez,[‡] and Ana M. Rodríguez[‡]

The equimolecular reaction of high and low sterically hindered NNN'-heteroscorpionate protioligands with AlR_3 proceed to give the mononuclear dialkyl aluminum bidentate-acetamidinates $[AlR_2(\kappa^2\text{-}N'N')]$ or monodentate-acetamidinates $[AlR_2(\kappa^2\text{-}NN')]$, respectively. A very unusual ligand exchange process takes place when several aluminum dimethyls react with $ZnMe_2$. DFT calculations justified the favored stability of all families. These aluminum dialkyls act as efficient living initiators for the immortal ROP of *rac*-LA with enriched levels of heteroselectivity ($P_s = 0.70$).

High sterically hindered enviroment

18 h, 50 ˚C
49% conv
rac-LA
$P_s = 0.70$

+ 20 equiv. BnOH
inmortal conditions
4 h, 70 ˚C
98% conv
rac-LA
$P_s = 0.66$

$[rac\text{-LA}]_0/[Al]_0 = 200$
Heterotactic-enriched PLA

18 h, 50 ˚C
47% conv
$P_s = 0.65$
rac-LA

Tautomer CH + *Tautomer NH*

Low sterically hindered enviroment

FOR TABLE OF CONTENTS USE ONLY